

Twist-bend nematic liquid crystals in high magnetic fields

P. K. Challa,¹ V. Borshch,² O. Parri,³ C. T. Imrie,⁴ S. N. Sprunt,¹ J. T. Gleeson,¹ O. D. Lavrentovich,² and A. Jákli²

¹*Department of Physics, Kent State University, Kent, Ohio 44242, USA*

²*Liquid Crystal Institute and Chemical Physics Interdisciplinary Program, Kent State University, Kent, Ohio 44242, USA*

³*Merck Chemicals Ltd., Chilworth Technical Centre, University Parkway, Southampton SO16 7QD, United Kingdom*

⁴*Department of Chemistry, School of Natural and Computing Sciences, University of Aberdeen, Aberdeen AB24 3UE, Scotland*

(Received 17 December 2013; published 6 June 2014)

We present magneto-optic measurements on two materials that form the recently discovered twist-bend nematic (N_{tb}) phase. This intriguing state of matter represents a fluid phase that is orientationally anisotropic in three directions and also exhibits translational order with periodicity several times larger than the molecular size. N_{tb} materials may also spontaneously form a visible, macroscopic stripe texture. We show that the optical stripe texture can be persistently inhibited by a magnetic field, and a 25 T external magnetic field depresses the N - N_{tb} phase transition temperature by almost 1°C. We propose a quantitative mechanism to account for this shift and suggest a Helfrich-Hurault-type mechanism for the optical stripe formation.

DOI: [10.1103/PhysRevE.89.060501](https://doi.org/10.1103/PhysRevE.89.060501)

PACS number(s): 61.30.Cz, 64.70.M-, 61.30.Jf

A nematic (N) liquid crystalline (LC) phase of achiral rod-shaped molecules is characterized by a long-range orientational and short-range positional order where the direction of the long axis of single molecules is parallel to the optical axis of the medium [1]. An existence of a “twist-bend” (tb) nematic phase in which the molecular director exhibits periodic twist and bend deformations following the line of an oblique helicoid, with the optical axis being the axis of the helicoid, was also proposed a long time ago by Meyer [2] and in subsequent theoretical and simulation works [3–6]. Recently, dimeric compounds formed by two rigid rodlike cores linked together by a flexible aliphatic chain with odd numbered carbon atoms were found to show a transition from a nematic phase to a birefringent striped phase [7] with periodicity in the micron range. This state was originally identified as a smectic- A phase [8], but x-ray studies have since ruled this out [9] and the striped state was tentatively labeled as an “ N_x ” phase [7]. ^2H nuclear magnetic resonance spectroscopy showed that the N_x phase has local chiral order [10–12], although the compounds are *achiral*. N_x phase recently was also found in chiral and doped dimers [13,14]. Freedericksz transition measurements and dynamic light scattering revealed an unusually low bend elastic constant in the nematic phase just above the N - N_x phase transition [15,16]. The N_x phase also exhibits linear (polar) switching under applied electric fields with a few microseconds response time [17,18], which was attributed to a twist-bend structure with a periodicity of a few molecular lengths (~ 10 nm) [19]. The surprisingly small length scale was indeed directly demonstrated via freeze fracture transmission electron microscopy (FFTEM) [16,20] to be 8–9 nm. The FFTEM textures also reveal distinctive, asymmetric Bouligand arches, verifying that the nanoscale periodic structure is indeed formed by twist-bend deformations of the molecular director [16].

Although the N_x phase has now been positively identified as the twist-bend nematic (N_{tb}) phase (observed also in rigid bent-core material [20]), important open questions remain. Among these are the origin of the macroscopic (optical) stripe pattern and the magnitude and behavior of the elastic constants of the N_{tb} phase. In this Rapid Communication we present high field magneto-optic studies of two liquid crystals exhibiting

the N_{tb} phase. We demonstrate that a large magnetic field can suppress the N - N_{tb} transition temperature by almost 1°C, and a sufficiently large field can persistently remove the optical stripe texture. We propose a coarse-grain model to explain the optical stripes and to estimate the elastic constants of the N_{tb} phase.

We studied two materials: (1) KA(0.2), which is a six-component formulation with 20 mol % methylene linked dimer 1'',9''-bis(4-cyano-2'-fluorobiphenyl-4'-yl)nonane (CBF9CBF) added to a base mixture composed of five odd-membered liquid crystal dimers with ether linkages containing substituted biphenyl mesogenic groups [15]; and (2) CB7CB, which is a single-component compound 1'',7''-bis(4-cyanobiphenyl-4'-yl)heptane [8]. The N - N_{tb} transition temperatures are 37.4 and 103.4°C for KA(0.2) and CB7CB, respectively. The materials were loaded into glass sandwich cells treated for planar alignment with cell spacing $d = 10$ μm [KA(0.2)] or 5 μm (CB7CB). The cells were held in a temperature controlled oven which was placed at the center of the vertical bore of the 25 T split-helix resistive solenoid magnet [21] at the National High Magnetic Field Laboratory (NHMFL).

The two materials were studied using the optical arrangement depicted in Fig. 1. This setup allows us to directly measure the phase difference, $\varphi = 2\pi \Delta n_{\text{eff}} d / \lambda$, where Δn_{eff} is the effective birefringence of the sample [22,23]. The optical stripe pattern, when present, acts as a diffraction grating; a detector (D1 in Fig. 1) is positioned at the first diffraction maximum to monitor the presence of these stripes. The temperature dependencies of the diffracted intensity (I_D) at zero and 25 T magnetic fields is shown in Fig. 2(a) and the magnetic-field dependencies at fixed temperatures is shown in Fig. 2(b).

As shown in Fig. 2(a), in both materials and in zero applied field, I_D increases dramatically at the N - N_{tb} phase transition. The optical stripes producing the diffraction are very regular in KA(0.2), and the diffraction spots are clearly defined up to the sixth order [see inset in Fig 4(a)]. In CB7CB the stripes are more complex, and in addition to the clearly visible “macroscopic” stripes with a period comparable to the film thickness, one also observes a micron width stripe tilted

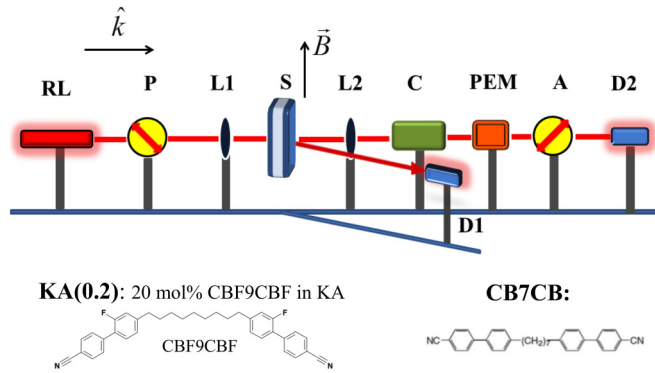


FIG. 1. (Color online) Schematic of the optical setup and molecular structures of the materials KA(0.2) and CB7CB. RL: 30 mW $\lambda = 632.8$ nm He-Ne laser; S: LC sample placed between crossed polarizers (P and A) oriented at $\pm 45^\circ$ with respect to the vertical magnetic field; L1 and L2 are +500 mm focal length lenses focusing the laser spot to ~ 50 μm diameter. C: A compensator to correct for residual birefringence; PEM: photoelastic modulator; D1 and D2: Photodetectors positioned at the first order diffraction maximum and the direct beam, respectively.

with respect to the macroscopic stripes and often intercalated with arrays of focal conic domains [see Fig. 4(b)]. When the samples cooled through the transition at 25 T I_D remains at least 100 times lower than recorded when the stripe texture is present in zero field.

As the field is ramped up at a rate of 5 T/min at fixed temperatures below the $N-N_{\text{tb}}$ transition [Fig. 2(b)] I_D dramatically decreases at a temperature-dependent threshold field. In KA(0.2) the threshold field needed to suppress the stripes increases with decreasing temperature below the (zero-field) $N-N_{\text{tb}}$ transition. Interestingly at lower temperatures there is first an increase in I_D before it drops to background levels. In CB7CB at 2 $^\circ\text{C}$ below the transition, a much larger magnetic field was required to completely suppress the stripes. When the field is subsequently removed (at fixed temperature), the stripes only slightly appear again even after several hundred seconds have elapsed.

The temperature and magnetic-field dependencies of the effective birefringence Δn_{eff} of both materials are non-monotonous and rather complex (see Fig. 3), as they are expected to depend at least on four factors: (i) changes of the degree of orientational order, (ii) pretransitional fluctuations, (iii) formation of heliconical N_{tb} structure, and (iv) formation of the stripe pattern with a distorted helicoidal axis. Figure 3(a) shows the variation of Δn_{eff} at the function of relative temperature with respect to $N-N_{\text{tb}}$ transition upon cooling at a rate of 1 $^\circ\text{C}/\text{min}$. In zero field Δn_{eff} of both materials have maxima at 3–4 $^\circ\text{C}$ above the $N-N_{\text{tb}}$ transition, then decrease slightly till the transition [37.4 $^\circ\text{C}$ for KA(0.2) and 103.4 $^\circ\text{C}$ for CB7CB]. At the transition when the optical stripes appear, Δn_{eff} decreases much more rapidly: without a discontinuous jump for KA(0.2), and with an abrupt drop by 0.03 for CB7CB. These indicate a second (or weak first), and a first order transition, respectively. When the sample is cooled under a 25 T field, which aligns the optic axis in both phases uniformly, the true birefringence Δn is obtained. The values of Δn_{eff} then drop abruptly by ~ 0.05 at 1 and 0.7 $^\circ\text{C}$ lower than measured

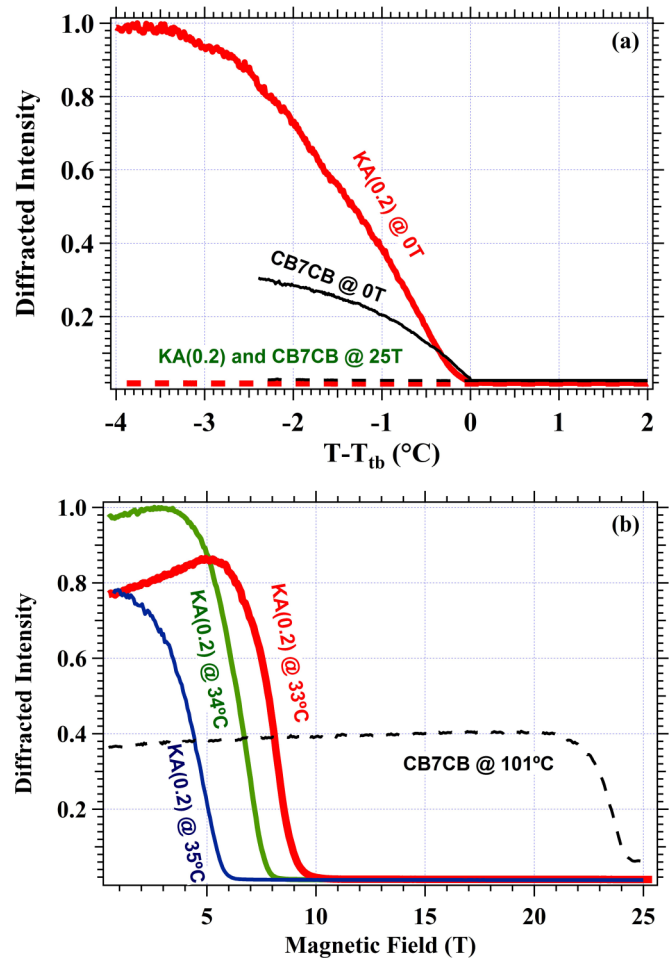


FIG. 2. (Color online) Temperature and magnetic-field dependence of the light intensity measured at the first diffraction peak. (a) Temperature dependencies for KA(0.2) and CB7CB at 0 and 25 T. (b) Magnetic-field dependencies for KA(0.2) at 33, 34, and 35 $^\circ\text{C}$ and for CB7CB at 101 $^\circ\text{C}$.

at zero field for KA(0.2) and CB7CB, respectively. These show that the high magnetic field depresses the $N-N_{\text{tb}}$ phase transitions. Below these transitions the birefringence is only weakly temperature dependent.

Figure 3(b) shows the magnetic-field dependencies of Δn_{eff} in the N_{tb} phase after it was cooled at zero field below the $N-N_{\text{tb}}$ phase transition. Solid lines show the behavior for KA(0.2) at three constant temperatures, and the dashed line represents the variation for CB7CB at 2.4 $^\circ\text{C}$ below the transition. For KA(0.2) the measured Δn_{eff} increases strongly above 3, 5, and 8 T and saturates above 8, 10, and 12 T at 35, 34, and 33 $^\circ\text{C}$, respectively. For CB7CB at $T = 101$ $^\circ\text{C}$ Δn_{eff} increases slowly as the field is ramped up to about 20 T, and then quite sharply between 22 and 24 T. The saturated birefringence for both materials is smaller in the N_{tb} than in the N phase. When the field is ramped back down to zero, the birefringence decreases only slightly and remains well above the original zero-field value [see inset to Fig 3(b) for KA(0.2)].

The depressions of the $N-N_{\text{tb}}$ transition temperatures by the 25 T field are due to the positive diamagnetic anisotropy, $\Delta\chi_N$. High field aligns the director uniformly and hence stabilizes

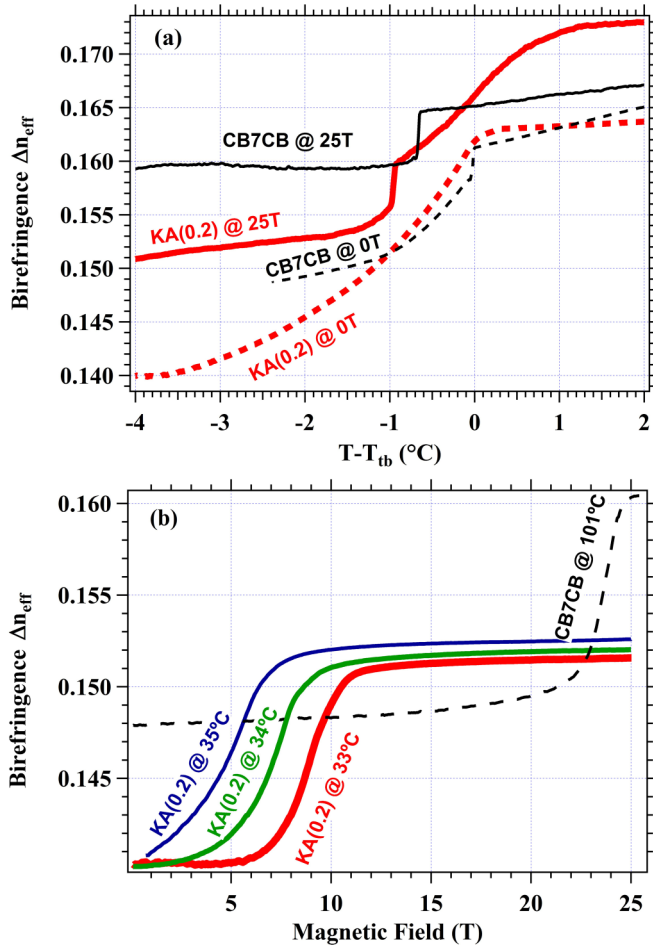


FIG. 3. (Color online) Effective birefringence measurements for both materials. (a) Temperature dependence at 0 and 25 T on cooling at $1^{\circ}\text{C}/\text{min}$ rate. (b) Magnetic-field dependencies (inset shows the results in decreasing fields).

the N phase to temperatures lower than the zero-field transition temperature. The shift of the transition temperature, ΔT , induced by the magnetic induction \vec{B} , can be estimated using the modified Kirkwood-Helfrich equation [24]: $\frac{\Delta T}{T_0} \frac{L_m \rho}{M_m} \approx \frac{\Delta \chi_N}{2\mu_0} |\vec{B}|^2$. Here T_0 is the zero-field transition temperature in Kelvin, M_m is the molar mass, L_m is the latent heat of the transition, $\rho \sim 10^3 \text{ kg/m}^3$ is the mass density, and $\mu_0 = 4\pi \times 10^{-7} \text{ Vs/(Am)}$. For CB7CB $\Delta \chi_N$ should be close to that of pentyl-cyanobiphenyl (5CB), which is $\sim 10^{-6}$ in SI [25]. Using an estimate of $L_m \sim 100 \text{ J/mol}$ from heat capacity measurements [9], we arrive at $\Delta T \sim 1^{\circ}\text{C}$, which is close to the measured 0.7°C shift. The value of $\Delta \chi_N$ is not presently available for KA(0.2), although it should not be too different than that for CB7CB.

Measurements of Δn in both phases allow us to estimate the helicone angle θ_0 from the relation $\Delta n_{\text{tb}} \approx \Delta n_N (1 - \frac{3}{2}\theta_0^2)$ [16], where Δn_{tb} and Δn_N can be determined from Δn_{eff} measured in 25 T that eliminated the optical stripes. By using the Δn_N values [0.173 for KA(0.2) and 0.167 for CB7CB] measured before the pretransitional decrease, and Δn_{tb} measured 0.5°C below the N - N_{tb} transition [0.153 for

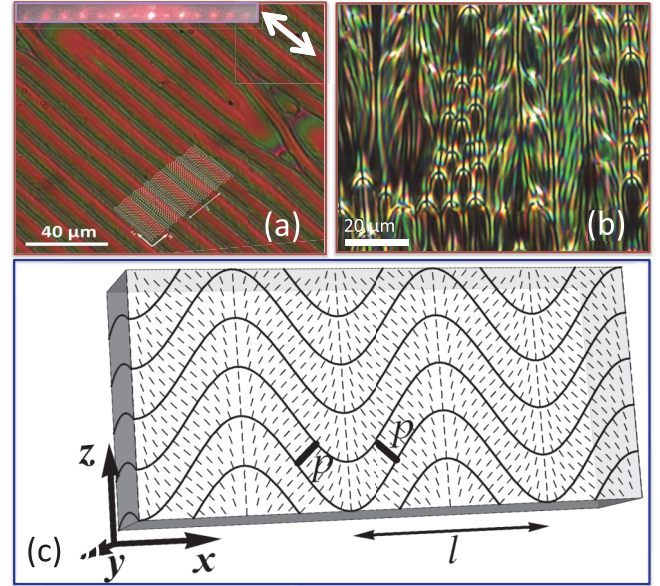


FIG. 4. (Color online) Illustration and model of the optical stripes. (a) Optical texture of a $10\text{-}\mu\text{m}$ -thick film of KA(0.2) with planar anchoring between crossed polarizers parallel to the edges of the picture. The white arrow indicates the rubbing direction. Inset on top shows the diffraction pattern, and the dotted white lines indicate the modulation of the helical axis. (b) Optical texture of a $10\text{-}\mu\text{m}$ -thick film of CB7CB. (c) Illustration of the undulation of the pseudolayers determined by the pitch of the conical helix of pitch p . Due to the undulation the direction of the helicoidal axes (short lines) are periodically changing in the x direction by a period l .

KA(0.2) and 0.159 for CB7CB], we find $\theta_0 \approx 16^{\circ}$ for KA(0.2) and $\theta_0 \approx 10^{\circ}$ for CB7CB.

The textures of stripes and focal conic domains are ubiquitous in systems such as smectics and cholesterics, formed by one-dimensional stacking of flexible equidistant layers [1,26]. They indicate the tendency of layers to tilt in response to a mechanical stress [26], such as the temperature-induced variation of the period. The underlying physics is captured well by the so-called Helfrich-Hurault (HH) buckling instability [1], which usually is described for the geometry in which the layers are parallel to the bounding plates of the cell, however, the general mechanism of the HH buckling remains valid even when the layers are perpendicular to the bounding plates. In such “bookshelf” geometry, the tilt of smectic layers typically occurs across the cell (vertical chevron) [27], but it is also observed in the plane of the cell [27–29]. The latter “horizontal chevron” texture is similar to the optical stripes observed in N_{tb} that, thanks to the nanoscale twist-bend deformations, also has a pseudolayer structure. The optical stripes shown in Figs. 4(a) and 4(b) are parallel to the average optical axis, and the period of undulating stripe patterns proportional to the cell thickness [6], just as established for a smectic C in the bookshelf geometry [26]. We use the HH-buckling framework to analyze the magnetic-field-induced elimination of the optical stripes and to estimate elastic properties of N_{tb} .

We assume that the displacement of the undulating pseudolayers of the N_{tb} phase has the form $u = u_0 \sin(q_z z) \cos(q_x x)$, where the z axis is parallel to the stripes (helical axis of a

uniform state) and the x axis is directed perpendicularly to the stripes [Fig. 4(c)].

The “coarse-grain” model of N_{tb} with weakly distorted pseudolayers is described by the energy density functional

$$F_{\text{cg}} = \frac{1}{2}B \left[\frac{\partial u}{\partial z} - \frac{1}{2} \left(\frac{\partial u}{\partial x} \right)^2 \right]^2 + \frac{1}{2}K \left(\frac{\partial^2 u}{\partial x^2} \right)^2 - \frac{1}{2} \frac{\Delta\chi_{\text{tb}} |\vec{B}_c|^2}{\mu_0}. \quad (1)$$

Here B is the layer compression modulus, K is the effective splay constant for the helicoidal axis, and $\Delta\chi_{\text{tb}} = \Delta\chi_N(3\cos^2\theta_0 - 1)/2$ is the diamagnetic susceptibility anisotropy of N_{tb} . The HH relation describing the geometry of undulation is $q_x^2 = q_z/\lambda$, where $q_x = 2\pi/l$, l is the observed period of optical stripes, $\lambda = \sqrt{K/B}$ is the elastic extrapolation length, and q_z is set by a less known anchoring condition; its value does not enter directly into the numerical calculations below. The magnitude of the magnetic induction $|\vec{B}_c|$ that restores the flat configuration of layers can be determined by equating the magnetic and elastic energies in Eq. (1) [1]: $\Delta\chi_{\text{tb}} |\vec{B}_c|^2 / \mu_0 = 2q_x^2 K = 8\pi^2 K / l^2$. The experimental values of $|\vec{B}_c|$ for KA(0.2) are 4, 6.5, and 8 T at $T_{\text{tb}} - T = 2.4, 3.4,$ and 4.4 °C, respectively, and 23 T at $T_{\text{tb}} - T = 2.4$ °C for CB7CB [see Fig. 2(b)]. Since θ_0 is small $\Delta\chi_{\text{tb}} \sim \Delta\chi_N \sim 10^{-6}$ for both materials, and using the observed $l \sim 10$ μm for KA(0.2) and $l \sim 2$ μm for CB7CB, we find that K increases from 20 to about 80 pN, as the temperature decreases from $T_{\text{tb}} - T = 2.4$ to 4.4 °C for KA(0.2), and of $K \sim 25$ pN in CB7CB at $T_{\text{tb}} - T = 2.4$ °C. The experimental values $K \approx 20$ – 80 pN for the N_{tb} phase of KA(0.2) are higher than the splay elastic constant $K_1 \approx 15$ pN measured in the N phase of this material near the N - N_{tb} transition point [14], which is an expected result. It would be of interest to measure the compressibility modulus B in Eq. (1) directly, for example, by causing undulations of pseudolayers in dilated homeotropic samples, as described for smectic and cholesteric liquid crystals [30,31]. One would expect B in the N_{tb} phase to be smaller than its counterpart in the thermotropic

smectic liquid crystals, as the change in pseudolayer spacing implies essentially molecular realignments within the oblique helicoidal director configuration rather than a change in the molecular density.

There are two features of the N_{tb} phase that make the coarse-grained models such as Eq. (1) an attractive option for the description of deformed states of the N_{tb} phase, such as the striped textures or field-induced Frederiks transition involving splay and saddle-splay deformations, as discussed in Ref. [16]. First, the N_{tb} pitch ($p_0 \sim 10$ nm) [16,20] is very small, not much larger than the molecular length (~ 3 nm). Second, N_{tb} is expected to feature coexisting left- and right-hand twisted domains [3], which implies a presence of walls separating them [16] and thus spatial heterogeneity at various scales, from about 30 nm [16] to microns [18], depending on the sample and its prehistory.

In summary, we have demonstrated that a high magnetic field shifts the N - N_{tb} transition temperature and suppresses the micron-scale (“optical”) stripe patterns of the N_{tb} samples. We explain the optical stripes as undulations of the Helfrich-Hurault type inherent to other modulated liquid crystal phases, such as smectics and short-pitch cholesterics. The suppression of stripes by the magnetic field is explained by the coarse-grained model that treats the N_{tb} phase as a system of pseudolayers and allows us to estimate the splay elastic constant of the N_{tb} helicoidal axis that is a few times larger than the splay elastic constant of the corresponding nematic phase.

This work was supported by the NSF under Grants No. DMR-0964765, No. DMR-1104805, No. DMR-1121288, and No. DMR-1307674, as well as DOE Grant No. DE-FG02-06ER 46331. Invaluable assistance was provided by W. Aldhizer and S. W. McGill. Work performed at NHMFL was supported by NSF cooperative agreement DMR-0084173, the State of Florida, and the U.S. Department of Energy.

-
- [1] P. G. de Gennes and J. Prost, *The Physics of Liquid Crystals*, 2nd ed. (Clarendon, Oxford, 1993).
- [2] R. B. Meyer, in *Molecular Fluids*, Les Houches Lectures, edited by R. Balian and G. Weill (Gordon and Breach, Tokyo, 1973), pp. 271–343.
- [3] I. Dozov, *Europhys. Lett.* **56**, 247 (2001).
- [4] R. Memmer, *Liq. Cryst.* **29**, 483 (2002).
- [5] S. M. Shamid, S. Dhakal, and J. V. Selinger, *Phys. Rev. E* **87**, 052503 (2013).
- [6] E. G. Virga, *Phys. Rev. E* **89**, 052502 (2014).
- [7] V. P. Panov, M. Nagaraj, J. K. Vij, Y. P. Panarin, A. Kohlmeier, M. G. Tamba, R. A. Lewis, and G. H. Mehl, *Phys. Rev. Lett.* **105**, 167801 (2010).
- [8] P. J. Barnes, A. G. Douglass, S. K. Heeks, and G. R. Luckhurst, *Liq. Cryst.* **13**, 603 (1993).
- [9] M. Cestari, S. Diez-Berart, D. A. Dunmur, A. Ferrarini, M. R. de la Fuente, D. J. B. Jackson, D. O. Lopez, G. R. Luckhurst, M. A. Perez-Jubindo, R. M. Richardson, J. Salud, B. A. Timimi, and H. Zimmermann, *Phys. Rev. E* **84**, 031704 (2011).
- [10] J. W. Emsley, P. Lesot, G. R. Luckhurst, A. Meddour, and D. Merlet, *Phys. Rev. E* **87**, 040501 (2013).
- [11] J. W. Emsley, M. Lelli, A. Lesage, and G. R. Luckhurst, *J. Phys. Chem. B* **117**, 6547 (2013).
- [12] L. Beguin, J. W. Emsley, M. Lelli, A. Lesage, G. R. Luckhurst, B. A. Timimi, and H. Zimmermann, *J. Phys. Chem. B* **116**, 7940 (2012).
- [13] A. Zep, S. Aya, K. Aihara, K. Ema, D. Pocięcha, K. Madrak, P. Bernatowicz, H. Takezoe, and E. Gorecka, *J. Mater. Chem. C* **1**, 46 (2013).
- [14] R. J. Mandle, E. J. Davis, C. T. Archbold, S. J. Cowling, and J. W. Goodby, *J. Mater. Chem. C* **2**, 556 (2014).
- [15] K. Adlem, M. Čopič, G. R. Luckhurst, A. Mertelj, O. Parri, R. M. Richardson, B. D. Snow, B. A. Timimi, R. P. Tuffin, and D. Wilkes, *Phys. Rev. E* **88**, 022503 (2013).

- [16] V. Borshch, Y.-K. Kim, J. Xiang, M. Gao, A. Jákli, V. P. Panov, J. K. Vij, C. T. Imrie, M. G. Tamba, G. H. Mehl, and O. D. Lavrentovich, *Nat. Commun.* **4**, 2635 (2013).
- [17] V. P. Panov, R. Balachandran, M. Nagaraj, J. K. Vij, M. G. Tamba, A. Kohlmeier, and G. H. Mehl, *Appl. Phys. Lett.* **99**, 261903 (2011).
- [18] V. P. Panov, R. Balachandran, J. K. Vij, M. G. Tamba, A. Kohlmeier, and G. H. Mehl, *Appl. Phys. Lett.* **101**, 234106 (2012).
- [19] C. Meyer, G. R. Luckhurst, and I. Dozov, *Phys. Rev. Lett.* **111**, 067801 (2013).
- [20] D. Chen, J. H. Porada, J. B. Hooper, A. Klittnick, Y. Shen, M. R. Tuchband, E. Korblova, D. Bedrov, D. M. Walba, M. A. Glaser, J. E. Maclennan, and N. A. Clark, *Proc. Natl. Acad. Sci. U.S.A.* **110**, 15931 (2013).
- [21] P. K. Challa, O. Curtiss, J. C. Williams, R. Twieg, J. Toth, S. McGill, A. Jákli, J. T. Gleeson, and S. N. Sprunt, *Phys. Rev. E* **86**, 011708 (2012).
- [22] J. C. Kemp, *J. Opt. Soc. Am.* **59**, 950 (1969).
- [23] T. Ostapenko, C. Zhang, S. N. Sprunt, A. Jákli, and J. T. Gleeson, *Phys. Rev. E* **84**, 021705 (2011).
- [24] W. Helfrich, *Phys. Rev. Lett.* **24**, 201 (1970).
- [25] A. Buka and W. H. de Jeu, *J. Phys.* **43**, 361 (1982).
- [26] M. Kleman and O. D. Lavrentovich, *Soft Matter Physics: An Introduction* (Springer, New York, 2003), p. 638.
- [27] A. Jákli and A. Saupe, *Phys. Rev. A* **45**, 5674 (1992).
- [28] Y. Ouchi, Y. Takanishi, H. Takezoe, and A. Fukuda, *Jpn. J. Appl. Phys.* **28**, 2547 (1989).
- [29] D. Subacius, D. Voloschenko, P. Bos, and O. D. Lavrentovich, *Liq. Cryst.* **26**, 295 (1999).
- [30] M. Delaye, R. Ribotta, and G. Durand, *Phys. Lett. A* **44**, 139 (1973).
- [31] N. A. Clark and R. B. Meyer, *Appl. Phys. Lett.* **22**, 493 (1973).